Identification of hub genes and transcription factor-miRNA-mRNA pathways in mice and human renal ischemia-reperfusion injury

Peng Ke[1], Lin Qian[1], Yi Zhou[2], Feng Liu[1], Zhentao Zhang[2], Chengjie Zheng[1], Mengnan Chen[1], Xinlei Huang[1], Xiaodan Wu[1]

[1] Department of Anesthesiology, Shengli Clinical Medical College, Fujian Medical University, Fuzhou, Fujian, China
[2] Institute of Pharmaceutics, College of Pharmaceutical Sciences, Zhejiang University, Hangzhou, Zhejiang, China

Corresponding Author:
Xiaodan Wu[1]
Department of Anesthesiology, Shengli Clinical Medical College, Fujian Medical University, Fuzhou, Fujian, 350001, China
Email address: wxiaodan@sina.com

Abstract

42

43   **Background.** Renal ischemia-reperfusion injury (IRI) is a disease with high incidence rate in
44   kidney related surgery. Micro RNA (miRNA) and transcription factors (TFs) are widely involved
45   in the process of renal IRI through regulation of their target genes. However, the regulatory
46   relationships and functional roles of TFs, miRNAs and mRNAs in the progression of renal IRI
47   are insufficiently understood. The present study aimed to clarify the underlying mechanism of
48   regulatory relationships in renal IRI.

49   **Methods.** Six gene expression profiles were downloaded from Gene Expression Omnibus
50   (GEO). Differently expressed genes (DEGs) and differently expressed miRNAs (DEMs) were
51   identified through RRA integrated analysis of mRNA datasets (GSE39548, GSE87025,
52   GSE52004, GSE71647, and GSE131288) and miRNA datasets (GSE29495). miRDB and
53   TransmiR v2.0 database were applied to predict target genes and TFs of miRNA, respectively.
54   DEGs were applied for Gene Ontology (GO) and Kyoto Encyclopedia of Genes and Genomes
55   (KEGG) analysis, followed with construction of protein-protein interaction (PPI) network. Then,
56   TF-miRNA-mRNA network was constructed. Correlation coefficient and ROC analysis were
57   used to verify regulatory relationship between genes and their diagnostic value in GSE52004.
58   Furthermore, in independent mouse RNA-seq datasets GSE98622, human RNA-seq GSE134386
59   and *in vitro*, the expression of hub genes and genes from the network were observed and
60   correlation coefficient and ROC analysis were validated.

61   **Results.** A total of 21 DEMs and 187 DEGs were identified in renal IRI group compared to
62   control group. The results of PPI analysis showed 15 hub genes. The TF-miRNA-mRNA
63   regulatory network was constructed and several important pathways were identified and further
64   verified, including Junb-miR-223-Ranbp3l, Cebpb-miR-223-Ranbp3l, Cebpb-miR-21-Ranbp3l
65   and Cebpb-miR-181b-Bsnd. Four regulatory loops were identified, including Fosl2-miR-155,
66   Fosl2-miR-146a, Cebpb-miR-155 and Mafk-miR-25. The hub genes and genes in the network
67   showed good diagnostic value in mice and human.

68   **Conclusions.** In this study, we found 15 hub genes and several TF-miRNA-mRNA pathways,
69   which are helpful for understanding the molecular and regulatory mechanisms in renal IRI. Junb-
70   miR-223-Ranbp3l, Cebpb-miR-223-Ranbp3l, Cebpb-miR-21-Ranbp3l and Cebpb-miR-181b-
71   Bsnd were the most important pathways, while Spp1, Fos, Timp1, Tnc, Fosl2 and Junb were the
72   most important hub genes. Fosl2-miR-155, Fosl2-miR-146a, Cebpb-miR-155 and Mafk-miR-25
73   might be the negative feedback loops in renal IRI.

74

Introduction

76   Ischemia-reperfusion injury (IRI) is one of the main causes of acute kidney injury. Every year,
77   one in every 2000 people died of acute kidney injury caused by IRI (*Ali et al., 2007*). Renal IRI
78   usually occurs after kidney transplantation, causing renal tissue damage and fibrosis (*Menke et
79   al., 2014*), which plays adverse effects on the function of kidney and long-term prognosis of
80   patients (*Tilney & Guttmann, 1997*). So far, there has no effective treatment for renal IRI.

81   Transcription factors (TFs) are proteins that can bind to target DNA and regulate the
82   transcription level of target genes (*Hughes, 2011*). Many studies reported that TFs take part in
83   the biological process of renal IRI. Previous studies found that in the early stage of renal injury,
84   over expression of nuclear factor erythroid-2 related factor 2 (Nrf2) could delay the process of
85   renal tubular injury by inducing antioxidant enzymes and nicotinamide adenine dinucleotide
86   phosphate (NADPH) (*Nezu et al., 2017*). Other studies have found that transcriptional repressor
87   GATA binding 1 (Trps1) is an essential TF for the formation of epithelial cells in the process of
88   renal development, and the expression of Trps1 is positively correlated with the recovery of
89   kidney after IRI. This suggests that Trps1 is a potential target for the treatment of renal ischemia-
90   reperfusion injury (*Yang et al., 2017*). Recent studies have found that nicotiflorin can reduce the
91   apoptosis of HK-2 cells by binding with activating transcription factor 3 (Atf3), delaying the
92   process of renal IRI (*Lin et al., 2021*). In general, a considerable number of studies have shown
93   that TFs are important intermediate molecules in renal IRI.
94   MiRNA, a kind of endogenous non coding RNA with a length of about 22 nucleotides, can bind
95   to a variety of target mRNA and promote the degradation of target mRNA, inhibiting the
96   expression of target gene and participating in the regulation of a variety of biological functions
97   (*Ambros, 2014*). Previous studies showed that the expression of several miRNAs changed during
98   renal IRI, including miR-21, miR-20a, miR-146a, miR-199a-3p, miR-214, miR-192, miR-187,
99   miR-805 and miR-194 (*Godwin et al., 2010*). Other studies have found that miR-17-5p can
100   directly inhibit the expression of death receptor 6 to reduce apoptosis and delay the process of
101   renal IRI (*Hao et al., 2017*).
102   TF-miRNA-mRNA pathway is a kind of regulatory relationship and is crucial in the regulatory
103   mechanisms in renal IRI. Recent years, studies have been reported that TFs regulate the
104   expression of target genes through miRNAs in disease. However, the regulatory relationship of
105   TF-miRNA-mRNA network in renal IRI is still unclear. In this study, we integrated analysis of 6
106   datasets from GEO database to provide a comprehensive understanding of renal IRI. The target
107   genes and TFs of DEMs were predicted through online databases. Next, functional enrichment
108   analysis of DEGs were applied and the hub genes in the PPI network were identified, followed
109   with construction of TF-miRNA-mRNA network associated with renal IRI. Finally, the
110   regulatory relationship and diagnostic value of genes were verified, which help to clarify the
111   mechanisms and provide potential targets for renal IRI.
112

113   Materials & Methods

114   Collection of datasets

115   The mRNA expression profiles (GSE39548 (*Correa-Costa et al., 2012*), GSE52004 (*Liu et al.,*
116   *2014*), GSE71647 (*Nezu, Suzuki & Yamamoto, 2017*), GSE87025 (*Markó et al., 2016*) and
117   GSE131288 (*Aufhauser et al., 2021*)) and the miRNA expression profile (GSE29495 (*Shapiro et*
118   *al., 2011*)) datasets were downloaded from the GEO database (*http://www.ncbi.nlm.nih.gov/geo/*)
119   (*Barrett et al., 2013*). All of the datasets included renal IRI groups and control groups. Each

120   group contained no less than 8 samples. Datasets were all available for download from GEO
121   database. Flowcharts of the study was shown in 'Fig. 1'.
122

DEGs and DEMs of renal IRI

124   The mRNA datasets were analyzed by NetworkAnalyst (*Zhou et al., 2019*) and normalized
125   before further analysis, followed with integrated analysis by "RobustRankAggreg" (RRA)
126   package to define RRA DEGs in 5 mRNA datasets. The miRNA expression profile GSE29495
127   was analyzed to obtain the DEMs. The screening criteria for DEGs and DEMs were $|log_2FC| \geq 1$
128   and FDR < 0.05.
129

DEGs enrichment analysis and construction of PPI network

131   Gene ontology (GO) and Kyoto Encyclopedia of Gene and Genome (KEGG) pathways of DEGs
132   were analyzed by Metascape (*Zhou et al., 2019*). DEGs list was submitted and analyzed as M.
133   musculus. The PPI network and hub genes could be obtained quickly after clicking on "Express
134   Analysis". Hub genes were defined according to the Molecular Complex Detection (MCODE)
135   algorithm, usually with degree cutoff ≥ 3, K-core ≥ 4 and other parameters set as default values
136   to identify densely connected network components, which were reported to have a higher
137   probability to participate in biological regulation and disease status (*Bader & Hogue, 2003*).
138

Prediction of differently expressed target genes and TFs of miRNA

140   The target genes of DEMs were predicted by online database miRDB (*Chen & Wang, 2020*),
141   which was based on thousands of miRNA-target interactions from high-throughput sequencing
142   experiments and machine learning methods. The differently expressed target genes were
143   obtained by overlapping DEGs and target genes of DEMs. The TransmiR v2.0 database (*Tong et*
144   *al., 2019*), a database contains 1,785,998 TF-miRNA regulations derived from ChIP-seq
145   evidence, was applied to predict TFs of DEMs for further overlapping with DEGs to obtain the
146   differently expressed TFs. Therefore, differently expressed target genes and TFs were obtained.
147

Construction of TF-miRNA-mRNA network

149   TF-miRNA-mRNA network was constructed based on differently expressed TFs, DEMs and
150   target genes. Nodes that did not participate in the TF-miRNA-mRNA pathways were excluded.
151   Then several important regulatory pathways were identified.
152

Diagnostic value of genes and correlation coefficient between genes

154   In order to further verify the regulatory relationship between genes in the TFs-miRNA-mRNA
155   network, correlation analysis was used in R software. Generally, $|r| > 0.3$ indicates a correlation
156   between TF and target gene. Besides, receiver operating characteristic curve (ROC curve) was
157   applied in GraphPad Prism 7.0 to verify the diagnostic value of genes from the network for renal
158   IRI. According to constructing of ROC model and calculating the area under the curve (AUC), it

159 can better evaluate whether hub genes could be used as biomarkers with high sensitivity and
160 specificity in IRI model. Usually, AUC>0.9 is considered to have good fitting effect in the model,
161 which indicates that this gene has a good value in the diagnosis of diseases. GSE52004 datasets
162 were set as the training data.
163

164 **Verification of the renal IRI associated hub genes and their diagnostic value**
165 **through the analysis of RNA-seq data from mice and human**
166 To verify the reliability of the experimental results, another independent RNA-seq datasets,
167 GSE98622, was used to validate the expression of hub genes and their diagnostic value. RNA-
168 seq data have the characteristics of more accurate, which makes our results more credible.
169 GSE98622 was downloaded from GEO database and analyzed by NetworkAnalyst. 13 samples
170 were excluded for quality control. Finally, 36 samples were included for further correlation
171 analysis and ROC analysis. To verify the clinical value of the results, another human RNA-seq
172 datasets GSE134386 were also applied to verify the expression of genes. GSE134386 contains 9
173 expanded criteria donor samples and 8 living donor samples. The former kidneys experienced
174 longer ischemia time in comparison with the latter ones. Finally, The Human Protein Atlas,
175 available from *http://www.proteinatlas.org*, was applied to explore the expression of two target
176 genes (*Thul PJ et al., 2017*).
177

178 **The culturing of HK-2 cells and HR model**
179 Human kidney 2 (HK-2), a proximal convoluted tubular epithelial cell, derived from normal
180 kidney and were purchased from Procell Biotechnology Co. Ltd. (Procell). Cells were cultured in
181 DMEM/F12 medium (BI) contained 10% fetal bovine serum (Giboco) and 1% penicillin
182 streptomycin (Hyclone). The establishment of HR (hypoxia-reoxygenation) model was as follow
183 (*Wu et al., 2016*). Hypoxia (1% oxygen) was performed in hypoxia chamber for 24 hours after
184 the medium was replaced with serum-free DMEM/F12 medium, and then incubated under
185 normoxic conditions for 12 hour. To determine the effect of Cebpb on Bsnd and Ranbp3l, Cebpb
186 knockdown by siRNA for 12 hours before HR.
187

188 **Real-time fluorescence quantitative PCR**
189 Total RNA was extracted from HK-2 cells using EasySpin Plus Cell/Tissue RNA Rapid
190 Extraction Kit (Adlai). PCR primers were designed and synthesized (Supplementary file 9). RT-
191 qPCR was performed on Lightcycle480 (Roche) using the SYBR Premixex Taq II (2X)
192 (TAKARA). Fusion curves were performed after RT-qPCR to validate individual transcripts. All
193 the reactions were repeated three times and the data were analyzed using the 2-ΔΔCT method.
194 GAPDH was used as an internal control. The experiment was repeated three times independently.
195

196 **Statistical analysis**

197 Statistical analysis was performed by using NetworkAnalyst and R software. Numerical data
198 were presented as the mean ± standard deviation. DEGs and DEMs were calculated in
199 NetworkAnalyst and defined according to the criteria of $|\log_2FC| \geq 1$ and FDR ≤ 0.05.
200

Results

Expression profiles of mRNA and miRNA

203 The mRNA expression profiles were from five datasets, including GSE39548, GSE52004,
204 GSE71647, GSE87025 and GSE131288. The miRNA expression profile was from GSE29459.
205 There were 127 samples in mRNA expression profiles, including 69 renal IRI samples and 58
206 control samples. There were 16 samples in miRNA expression profile, including 8 renal IRI
207 samples and 8 control samples (Table 1). The raw measurements were provided in the
208 'Supplementary file 1'.
209

Identification of DEMs and DEGs

211 The data distribution of each datasets were uniform after normalization. Boxplot and PCA
212 showed that the qualified data can be used for further analysis (Supplementary file 2). Compared
213 with the control groups, 21 DEMs were identified in renal IRI groups, including 14 up-regulated
214 miRNAs and 7 down-regulated miRNAs (Fig. 2A). After obtaining the DEGs of each mRNA
215 gene expression profiles, 187 RRA DEGs were obtained by RRA integrated analysis, including
216 135 up-regulated genes and 52 down-regulated genes (Supplementary file 3). The top ten up-
217 regulated genes and the top ten down-regulated genes were shown in 'Fig. 2B'.
218

GO and KEGG pathway analysis on DEGs and PPI network

220 GO and KEGG analysis of RRA DEGs were performed in Metascape. In the GO and KEGG
221 analysis of DEGs, positive regulation of cell migration and TNF signaling pathway were
222 significantly enriched. Interestingly, some GO items related to transcription factors had also been
223 significantly enriched, including regulation of transcription from RNA polymerase Ⅱ promoter
224 in response to stress and transmembrane receptor protein tyrosine kinase signaling pathway (Fig.
225 3A). All of the enrichment items were closely related, indicating that the pathogenesis of the
226 renal IRI is complex (Fig. 3B). The PPI network showed 3 important MCODE modules (Fig.
227 3C), including 15 hub genes (Fig. 3D). Enrichment analysis on hub genes also showed that TNF
228 signaling pathway was significantly enriched (Supplementary file 4).
229

Prediction of TFs and miRNA target genes

231 274 TFs were predicted by TransmiR v2.0 database based on miRNA-target interactions from
232 high-throughput sequencing experiments (Supplementary file 5), of which 13 differently
233 expressed TFs were obtained by overlapping with DEGs (Fig. 4A). Based on this, regulatory
234 network of TF-miRNA was constructed and showed 15 miRNAs regulated by 13 TFs 3 down-
235 regulated miRNAs, including miR-455, miR-192 and miR-188-5p, were inconsistent with the

236   regulation of TF activate miRNA (Supplementary file 6). The results of miRDB showed that
237   6967 target genes were obtained (Supplementary file 7), of which 68 genes were consistent with
238   the DEGs (Fig. 4B). Among them, six target genes were TFs and marked in red. Therefore,
239   regulatory network of miRNA-mRNA was constructed, which contains 12 miRNAs and 17
240   down-regulated targets (Supplementary file 6).
241
242   **Construction of TF-miRNA-mRNA network**
243   The TF-miRNA-mRNA network consists of 11 transcription factors (Egr1 and Nfil3 were
244   deleted because they did not participate in the network), 10 miRNAs (miR-132 and miR-146a
245   were deleted because they had no corresponding down-regulated target genes) and 17 target
246   genes (Fig. 4C). Among them, Junb, Fos, Fosl1 and Fosl2 were hub genes, which showed their
247   important roles in the network. In addition, outside of this network, we found four regulatory
248   loops, including Fosl2-miR-155-Fosl2, Fosl2-miR-146a-Fosl2, Cebpb-miR-155-Cebpb and
249   Mafk-miR-25-Mafk (Table. 2), which indicated that TFs might maintain itself at a stable level
250   through their target miRNAs.
251
252   **Diagnostic value of genes and Correlation coefficient between genes**
253   In the TF-miRNA-mRNA network, we constructed a correlation analysis to show the correlation
254   between various genes. The regulatory relationship we concerned were framed in red and blue.
255   The red frames indicate that the correlation is satisfied. Atf4, Fosl1, Junb, Fosl2, Egr2 and Cebpb
256   were correlated with target genes ($|r| > 0.3$, $p < 0.05$) (Fig. 5A). Among them, Junb, Fosl1 and
257   Fosl2 were hub genes, which showed their important roles in the network again. ROC curve
258   showed that TFs and target genes from the network had a good accuracy in distinguishing renal
259   IRI and control mice as well as the hub genes (Fig. 5B).
260
261   **Verification of the renal IRI associated hub genes and diagnostic value of**
262   **target genes through the analysis of RNA-seq data from mice and human**
263   RNA-seq data GSE98622 was performed to verify the expression levels of 15 hub genes and
264   genes from the network. As shown in the analysis results, Timp1, Spp1, Csf1, Tnc, Junb, Fosl1,
265   Fos, Fosl2 and Akr1b8 were up-regulated genes in renal IRI. While Itih2, Igfbp5 and Akr1c18
266   were down-regulated in renal IRI. The expression of Mapk6, Txnrd1 and Gnpda1 was not
267   statistically significant between renal IRI and control group. The expression of genes in
268   regulatory network were also verified in RNA-seq analysis. TFs, including Junb, Fos Fosl1,
269   Fosl2 and Egr2, were up-regulated in renal IRI. Although the expression of Cebpb was less than
270   one, the difference was statistically significant. The change of Atf4 was not significant. Cyp7b1,
271   A4gnt, Ranbp3l, Ass1, Acmsd, Bsnd and Galm were down-regulated target genes in renal IRI,
272   while other target genes were not significant (Fig. 6A). The results of ROC analysis showed that
273   most of hub genes shared good diagnostic value, although the expression of some genes changed
274   less than one. Several genes from the network that verified to be differently expressed, were all
275   proved to share good diagnostic value again (Fig. 6C). Correlation analysis showed good

276   correlation between differently expressed TFs and target genes from the network (Fig. 6B).
277   Consistent with the previous results of GSE52004, TFs, including Fosl1, Junb, Fosl2, Egr2 and
278   Cebpb, were negatively regulated with their corresponding target genes in GSE98622. However,
279   there was no correlation between Atf4 and target genes. Interestingly, Fos showed a correlation
280   with Ass1 and Crebl2, which was inconsistent with that in GSE52004. In human samples, hub
281   genes, including SPP1, FOS, TIMP1, TNC, FOSL2 and JUNB, were verified to be up-regulated
282   in severely damaged kidneys. In the regulatory network, EGR2 and FOS were significantly up-
283   regulated. CEBPB, FOSL2 and JUNB were also up-regulated, with the fold change varied
284   between 0.5 and 1. Expression of BSND and RANBP3L from network showed significantly
285   changed, which was consistent with the observation in GSE98622 (Fig. 6D). The Human Protein
286   Atlas showed that Bsnd and Ranbp3l were mostly expressed in normal human kidney tissues,
287   especially Bsnd is uniquely up-regulated in the kidney, which suggest their importance in
288   maintaining normal physiological function (Fig. 7A). The protein expression levels of Bsnd and
289   Ranbp3l were consistent with their mRNA expression (Supplementary file 8).
290   Immunohistochemical staining showed that Bsnd and Ranbp3l were highly expressed in normal
291   kidney tissues (Fig. 7B). The figures were downloaded from The Human Protein Atlas
292   (https://www.proteinatlas.org/ENSG00000164188-RANBP3L/tissue and
293   https://www.proteinatlas.org/ENSG00000162399-BSND/tissue).
294
295   **Verification of the genes from the network *in vitro***
296   The expression of Fos, Egr2, Junb, Fosl2, Cebpb, Bsnd and Ranbp3l were verified in HK-2 cells
297   *in vitro*. Fos, Egr2, Junb, Fosl2 and Cebpb were up-regulated in HR group, while Bsnd and
298   Ranbp3l were down-regulated (Fig. 7C). After knockdown of Cebpb, the expression of Cebpb
299   was down-regulated, while Bsnd and Ranbp3l were up-regulated (Fig. 7D).
300

Discussion

302   The incidence of renal IRI is increasing recent years. 15 to 20 minutes of ischemia is enough to
303   cause kidney damage because of abundant blood supply and high metabolism of kidney (*Schrier*
304   *& Wang, 2004*). Currently, lots of research found genetic alteration after renal IRI. Some
305   achievements have been made in genes expression modification (*Tobisawa et al., 2017*) and
306   molecular treatment (*Yip et al., 2015*). Previous microarray studies have often focused on the
307   role of a single molecule in renal IRI while ignoring the important regulatory relationship
308   between genes. Regulation of miRNAs and TFs on target genes in renal IRI still remain unclear.
309   In this study, five mRNA expression profiles were integrated to reduce interference factors,
310   which was better than single gene expression profile analysis. 21 DEMs and 187 DEGs were
311   identified. 15 hub genes were identified in renal IRI. Several differently expressed TFs and target
312   genes were predicted based on over lapping with DEGs, followed with the construction of TF-
313   miRNA-mRNA regulatory network. Finally, biological significance of these genes and the
314   regulatory relationship between TFs and mRNAs were verified by the independent RNA-seq
315   datasets GSE98622, human datasets GSE134386 and *in vitro*.

316 Several DEMs were up-regulated in our result and have been reported in renal IRI. Some of the
317 DEMs have shown to alleviate kidney injury. MiR-21 in exosomes inhibited programmed cell
318 death protein 4 (PDCD4) and reduced apoptosis of tubular epithelial cell (*Du et al., 2020*). MiR-
319 146b, targeting interleukin (IL)-1 receptor-associated kinase (IRAK1), could reduce sepsis-
320 associated acute kidney (*Zhang et al., 2020*). Exosomes delivering miR-223 down-regulated
321 NLR Family Pyrin Domain Containing 3 (NLRP3) (*Yuan et al., 2017*). Injection of exosomes
322 carried with miR-199-3p decreased the expression of semaphorin 3A (Sema3A), while activated
323 Akt and ERK signaling pathways (*Zhu et al., 2019*). Li Xirui et al found that miR-146a from
324 exosomes protect renal IRI in rats (*Li et al., 2020*). The up regulation of these miRNAs in our
325 study might be caused by the protective effect of the body. Some of the DEMs have been
326 demonstrated to exacerbate kidney injury. MiR-132 promote renal tubular apoptosis (*Yan et al.
327 2020*), which plays the same effect as miR-155 (*Wu et al., 2016*). MiRNA-214 represses
328 mitofusin-2 (*Yan et al., 2020*) and disrupts mitochondrial oxidative phosphorylation to promote
329 renal IRI (*Bai et al., 2019*). These results are consistent with the results of existing research,
330 which strengthen the reliability of our analysis results.
331 Among the down-regulated DEMs, some miRNAs play aggravating roles in renal IRI. For
332 example, MiR-377 aggravates renal IRI by inhibiting vascular endothelial growth factor
333 (VEGF). Inhibition of miR-377 improves kidney injury (*Liu et al., 2019*). miR-188 was reported
334 in ischemia-reperfusion injury of retinal ganglio cells (*Ge et al., 2020*). miR-31 was also up-
335 regulated in cardiac IRI (*Wang et al., 2015*). MiR-200a is often up-regulated in the early stage of
336 injury (*Sonoda et al., 2019*). Here, we found miR-200a was down-regulated in the study and
337 need more study to explore it. Conversely, some miRNAs play protective roles in IRI. MiR-192
338 was down-regulated in renal IRI, which was consistent with our results (*Zhang et al., 2017*).
339 MiR-187 inhibit apoptosis by targeting acetylcholinesterase (ACHE) in mouse podocyte (MPC-
340 5) cells, which was consistent with miR-187 agomir injection in mice (*Yue et al., 2019*). MiR-
341 455 was also associated with cerebral IRI (*Fan et al., 2021*).
342 Studies reported that miR-181b, miR-25, miR-342-3p, miR-374 and miR-15b were involved in
343 IRI but not in renal IRI. Therefore, their roles in renal IRI require further exploration. Besides,
344 miR-15b, miR-214, miR-25, miR-342-3p, miR-223, miR-31, miR-181b, miR-146b, miR-155
345 and miR-21 were in the TF-miRNA-mRNA network we built. In addition, miR-31 has never
346 been reported in IRI.
347 Construction of PPI network is very commonly used in transcriptome analysis. 15 hub genes,
348 including Timp1, Spp, Csf1, Itih2, Tnc, Igfbp5, Mapk6, Junb, Fosl1, Fos, Fosl2, Txnrd1,
349 Gnpda1, Akrlc18 and Akrlb8, were identified according to the application of MCODE algorithm.
350 A large number of studies have adopted the results of MCODE as hub genes for further analysis.
351 These hub genes have higher probability to participate in biological regulation and correlated
352 with renal IRI and could act as biomarkers, which might be applied to estimate the severity of
353 IRI and verify effectiveness of treatments. Several genes has been reported in renal IRI, which
354 indicate the accuracy of our analysis. Timp1 is the marker of renal injury (*Deng et al., 2021*). Fos
355 mRNA expression was rapidly and briefly up-regulated following renal ischemia (*Megyesi et al.,*

356   *1995*). Spp1mainly takes part in the process of osteoblast differentiation and inflammatory
357   response (*Srirussamee et al., 2019*). Cebpb activates miR-16 to promote renal injury (*Chen et al.,*
358   *2016*). Interestingly, 4 hub genes were in the TF-miRNA-mRNA network, including Junb, Fos,
359   Fosl1 and Fosl2. While the role of Junb and Fosl2 in renal IRI remains unclear.
360   In the results of genes enrichment analysis, we found DEGs were significantly enriched in TNF
361   and MAPK signaling pathway. All of them have been reported in renal IRI. The results of GO
362   analysis showed that regulation of transcription from RNA polymerase Ⅱ promoter in response
363   to stress and transmembrane receptor protein tyrosine kinase signaling pathway were
364   significantly enriched, indicating that DEGs in renal IRI were closely related to transcription
365   factors. Therefore, TFs of DEMs were predicted in the study. A total of 13 differently expressed
366   TFs were found, including Atf4, Cebpb, Egr1, Egr2, Fos, Fosl1, Fosl2, Junb, Mafk, Nfil3, Snai1,
367   Sox4 and Sox9, suggesting their important roles in renal IRI. When constructing TF-miRNA, 2
368   TFs and 3 miRNAs were deleted due to their inconsistent expression regulation. 2 miRNAs and
369   up-regulated targets were also deleted during the construction of miRNA-mRNA because of their
370   negative regulatory relationship.
371   Finally, the TF-miRNA-mRNA network was constructed, which consist of 11 TFs, 10 miRNAs
372   and 17 target genes. All miRNAs in the network were up-regulated DEMs in renal IRI, which
373   also surprised us. There might be three reasons. Firstly, almost all of the transcription factors we
374   predicted activate their target miRNAs, indicating that target miRNAs should be up-regulated.
375   Thus, 7 down-regulated miRNAs were no longer in our concern. Secondly, we did observe that
376   TF inhibited miRNA, such as Cebpb inhibited miR-146a. However, the expression of miR-146a
377   was actually up-regulated in IRI, which was contrary to their negative regulatory relationship.
378   Thirdly, we deleted the DEMs or DEGs that are not involved in TF-miRNA-mRNA network and
379   only showed the most important information. Correlation analysis showed that several regulatory
380   pathways were correlated, which were consistent with our prediction. Unexpectedly, the
381   expression of some other genes were correlated, possibly because they are regulated or affected
382   by other more complex mechanisms. For example, some TFs might binding to their target
383   mRNAs directly. Besides, ROC curves showed the diagnostic value of genes in the network. The
384   role of ROC analysis verified that these genes correlated with renal IRI and could act as
385   biomarkers or therapeutic targets, which might be applied to estimate the severity of IRI and
386   verify effectiveness of treatments. In addition, we also found four regulatory loops, including
387   Fosl2-miR-155-Fosl2, Fosl2-miR-146a-Fosl2, Cebpb-miR-155-Cebpb and Mafk-miR-25-Mafk.
388   Regulatory loop has been reported in liver ischemia-reperfusion injury (*Pan et al., 2020*). Our
389   results showed that transcription factors bind to the promoter of miRNA and induce miRNA
390   express, so as to form a negative feedback loop with TF and maintain the stability of their
391   expression level.
392   To verify our analysis results, RNA-seq data GSE98622 was applied for analyzing the
393   expression of genes, ROC values and correlation analysis between genes, showing good support
394   for our analysis results. Based on the results of GSE98622, regulatory relationships between TFs
395   and target genes were verified. Finally, to explore the value of these genes in clinical practice,

396 expression of hub genes and genes from network were analyzed in human. To our excitement,
397 the expression of 6 hub genes (SPP1, FOS, TIMP1, TNC, FOSL2 and JUNB) were significantly
398 up-regulated in more severely damaged kidneys, which was highly consistent with the results in
399 mice. The expression of 5 TFs (FOS, EGR2, JUNB, FOSL2 and CEBPB) and 2 target genes
400 (BSND and RANBP3L) were also significantly changed, indicating their importance in human
401 IRI. BSND and RANBP3L have never been reported in renal IRI. These results suggest that
402 these genes have great research value in humans. Many genes have no significance in human
403 samples, which may be caused by the differences of species. Based on the above results, we
404 consider Junb-miR-223-Ranbp3l, Cebpb-miR-223-Ranbp3l, Cebpb-miR-21-Ranbp3l and Cebpb-
405 miR-181b-Bsnd as the most important pathways, and Spp1, Fos, Timp1, Tnc, Fosl2, Junb, Egr2,
406 Cebpb, Bsnd and Ranbp3l as the most important genes. Thus, we verified the expression of Fos,
407 Egr2, Cebpb, Junb, Fosl2, Bsnd and Ranbp3l *in vitro*. Bsnd and Ranbp3l were mostly expressed
408 in normal human kidney tissues, which suggest their importance in maintaining normal
409 physiological function. Both of them were down-regulated after IRI, and were up-regulated after
410 knockdown of Cebpb in our study, because the decrease of Cebpb leads to the down-regulated of
411 its target miRNA (miR-223, miR-21 and miR-181b), the latter inhibit the expression of Bsnd and
412 Ranbp3l. The expression of Cebpb and target miRNA are up-regulated during renal IRI, and can
413 aggravate the damage, while Randp3l is down-regulated. Randp3l has been reported to play a
414 protective role in renal carcinoma (*Chernyakov et al., 2021*). Therefore, these regulatory
415 relationships are of great significance for further research, we would further confirm them
416 experimentally in the future.
417 In this study, we have taken many measures to ensure the reliability of the study. For example,
418 RRA algorithm was applied to integrated analysis on multiple datasets. All of the datasets were
419 from the same species and the data were normalized before further analyzed. Two independent
420 RNA-seq datasets and HK-2 cells were applied to verify our results. However, there are still
421 some limitations. Firstly, DEGs analysis would inevitably filter out some important genes with
422 small changes. Secondly, the model condition of renal IRI from different datasets are not exactly
423 the same. Thirdly, we didn't explore the specific molecular functions of these hub genes in renal
424 IRI. In addition, the construction of TF-miRNA-mRNA pathways network lost some hub genes
425 not associated with DEMs, but it can also filter out many gene not involved in TF-miRNA-
426 mRNA pathways regulation to make the analysis more convincing. Because of RNA-seq datasets
427 contain no miRNA results, the verification of miRNAs in the pathways was indirectly. Due to
428 the small sample size in human datasets, ROC analysis and correlation analysis are difficult to
429 carry out. Further experimental studies are needed to prove the relationship between TF-miRNA-
430 mRNA pathways and four negative feedback loops.
431
Conclusions
433 In summary, we present a bioinformatics analysis of mRNA and miRNA expression and
434 identified several hub genes, TF-miRNA-mRNA regulatory pathways and four negative

435 feedback loops that might play important roles in renal IRI, which provide potential therapeutic
436 targets and deeper understanding of genetic mechanism for renal IRI.
437

Acknowledgements
439 This work was supported by the Joint fund for research and development of high-level hospital
440 (No. 2017LHJJ10).

441

442

443

References
445   **Ali T, Khan I, Simpson W, Prescott G, Townend J, Smith W, Macleod A. 2007.**
446 Incidence and outcomes in acute kidney injury: a comprehensive population-based study. *J Am*
447 *Soc Nephrol* **18:** 1292-8 DOI:10.1681/ASN.2006070756.
448   **Ambros V. 2004.** The functions of animal microRNAs. *Nature* **431:** 350-5
449 DOI:10.1038/nature02871.
450   **Aufhauser DD, Hernandez P, Concors SJ, O'Brien C, Wang ZL, Murken DR,**
451 **Samanta A, Beier UH, Krumeich L, Bhatti TR., Wang YF, Ge GH, Wang LQ, Cheraghlou**
452 **S, Wagner FF, Holson EB, Kalin JH, Cole PA, Hancock WW, Levine MH. 2021.** HDAC2
453 targeting stabilizes the CoREST complex in renal tubular cells and protects against renal
454 ischemia/reperfusion injury. *Sci Rep* **11:** 9018 DOI:10.1038/s41598-021-88242-3.
455   **Bader GD, Hogue CWV. 2003.** An automated method for finding molecular complexes in
456 large protein interaction networks. *BMC Bioinformatics* **4**: 2 DOI:10.1186/1471-2105-4-2.
457   **Bai M, Chen HM, Ding D, Song RH, Lin JJ, Zhang YY, Guo Y, Chen S, Ding GX,**
458 **Zhang Y, Jia ZJ, Huang SM, He JC, Yang L, Zhang AH. 2019.** MicroRNA-214 promotes
459 chronic kidney disease by disrupting mitochondrial oxidative phosphorylation. *Kidney Int* **95:**
460 1389-1404 DOI:10.1016/j.kint.2018.12.028.
461   **Barrett T, Wilhite SE, Ledoux P, Evangelista C, Kim IF, Tomashevsky M, Marshall**
462 **K, Phillippy KH, Sherman PM, Holko M, Yefanov A, Lee H, Zhang N, Robertson CL,**
463 **Serova N, Davis S, Soboleva A. 2013.** NCBI GEO: archive for functional genomics data sets--
464 update. *Nucleic Acids Res* **41:** D991-5 DOI:10.1093/nar/gks1193.
465   **Chen HH, Lan YF, Li HF, Cheng CF, Lai PF, Li WH, Lin H. 2016.** Urinary miR-16
466 transactivated by C/EBPβ reduces kidney function after ischemia/reperfusion-induced injury. *Sci*
467 *Rep* **6:** 27945 DOI:10.1038/srep27945.
468   **Chen YH, Wang XW. 2020.** miRDB: an online database for prediction of functional
469 microRNA targets. *Nucleic Acids Res* **48:** D127-D131 DOI:10.1093/nar/gkz757.
470   **Chernyakov D, Groß A, Fischer A, Bornkessel N, Schultheiss C, Gerloff D, Edemir B.**
471 **2021.** Loss of RANBP3L leads to transformation of renal epithelial cells towards a renal clear
472 cell carcinoma like phenotype. *J Exp Clin Cancer Res* **40:** 226 DOI:10.1186/s13046-021-01982-
473 y.

474   **Correa-Costa M, Azevedo H, Amano MT, Gonçalves GM, Hyane MI, Cenedeze MA,**
475   **Renesto PG, Pacheco-Silva A, Moreira-Filho CA, Câmara NOS. 2012.** Transcriptome
476   analysis of renal ischemia/reperfusion injury and its modulation by ischemic pre-conditioning or
477   hemin treatment. *PLoS One* **7:** e49569 DOI:10.1371/journal.pone.0049569.
478   **Deng WM, Wei XL, Dong ZW, Zhang JH, Huang ZY, Na N. 2021.** Identification of
479   fibroblast activation-related genes in two acute kidney injury models. *PeerJ* **9:** e10926
480   DOI:10.7717/peerj.10926.
481   **Du T, Zhou J, Chen WX, Zhang XL, Ji TY, Liu J, Rong L, Wang LD, Zhou RJ, Ding**
482   **DG. 2020.** Microvesicles derived from human umbilical cord mesenchymal stem cells
483   ameliorate renal ischemia-reperfusion injury via delivery of miR-21. *Cell Cycle* **19:** 1285-1297
484   DOI:10.1080/15384101.2020.1748940.
485   **Fan Y, Wei LH, Zhang SJ, Song XY, Yang JQ, He XX, Zheng XZ. 2021.** LncRNA
486   SNHG15 Knockdown Protects Against OGD/R-Induced Neuron Injury by Downregulating
487   TP53INP1 Expression via Binding to miR-455-3p. *Neurochem Res* **46:** 1019-1030
488   DOI:10.1007/s11064-020-03222-9.
489   **Ge YN, Zhang R, Feng YQ, Li HL. 2020.** Mbd2 Mediates Retinal Cell Apoptosis by
490   Targeting the lncRNA Mbd2-AL1/miR-188-3p/Traf3 Axis in Ischemia/Reperfusion Injury. *Mol*
491   *Ther Nucleic Acids* **19:** 1250-1265 DOI:10.1016/j.omtn.2020.01.011.
492   **Godwin JG, Ge X, Stephan K, Jurisch A, Tullius SG, Iacomini J. 2010.** Identification of
493   a microRNA signature of renal ischemia reperfusion injury. *Proc Natl Acad Sci USA* **107:**
494   14339-44 DOI:10.1073/pnas.0912701107.
495   **Hao JL, Wei QQ, Mei SQ, Li L, Su YC, Mei CL, Dong Z. 2017.** Induction of
496   microRNA-17-5p by p53 protects against renal ischemia-reperfusion injury by targeting death
497   receptor 6. *Kidney Int* **91:** 106-118 DOI:10.1016/j.kint.2016.07.017.
498   **Hughes TR. 2011.** Introduction to "a handbook of transcription factors". *Subcell Biochem*
499   **52:** 1-6 DOI:10.1007/978-90-481-9069-0_1.
500   **Li XR, Liao J, Su XJ, Li WQ, Bi ZR, Wang JL, Su Q, Huang HT, Wei YC, Gao YF, Li**
501   **J, Liu LS, Wang CX. 2020.** miR-146a-5pHuman urine-derived stem cells protect against renal
502   ischemia/reperfusion injury in a rat model via exosomal which targets. *Theranostics* **10:** 9561-
503   9578 DOI:10.7150/thno.42153.
504   **Liu J, Krautzberger AM, Sui SH, Hofmann OM, Chen Y, Baetscher M, Grgic I,**
505   **Kumar S, Humphreys BD, Humphreys B, Hide WA, McMahon AP. 2014.** Cell-specific
506   translational profiling in acute kidney injury. *J Clin Invest* **124:** 1242-54 DOI:10.1172/JCI72126.
507   **Liu ZH, Yang Q, Wei QJ, Chang YL, Qu M, Yu LL. 2019.** The protective effect of miR-
508   377 inhibitor against renal ischemia-reperfusion injury through inhibition of inflammation and
509   oxidative stress via a VEGF-dependent mechanism in mice. *Mol Immunol* **106:** 153-158
510   DOI:10.1016/j.molimm.2018.12.028.
511   **Markó L, Vigolo E, Hinze C, Park JK, Roël G, Balogh A, Choi M, Wübken A,**
512   **Cording J, Blasig IE, Luft FC., Scheidereit C, Schmidt-Ott KM, Schmidt-Ullrich R, Müller**

513 **D. 2016.** Tubular Epithelial NF-κB Activity Regulates Ischemic AKI. *J Am Soc Nephrol* **27:**
514 2658-69 DOI:10.1681/ASN.2015070748.

515 **Megyesi J, Di MJ, Udvarhelyi N, Price PM, Safirstein R. 1995.** DNA synthesis is
516 dissociated from the immediate-early gene response in the post-ischemic kidney. *Kidney Int* **48:**
517 1451-8 DOI:10.1038/ki.1995.434.

518 **Menke J, Sollinger D, Schamberger B, Heemann U, Lutz J. 2014.** The effect of
519 ischemia/reperfusion on the kidney graft. *Curr Opin Organ Transplant* **19:** 395-400
520 DOI:10.1097/MOT.0000000000000090.

521 **Nezu M, Souma T, Yu L, Suzuki T, Saigusa D, Ito S, Suzuki N. 2017.** Yamamoto
522 Masayuki. Transcription factor Nrf2 hyperactivation in early-phase renal ischemia-reperfusion
523 injury prevents tubular damage progression. *Kidney Int* **91:** 387-401
524 DOI:10.1016/j.kint.2016.08.023.

525 **Nezu M, Suzuki N, Yamamoto M. 2017.** Targeting the KEAP1-NRF2 System to Prevent
526 Kidney Disease Progression. *Am J Nephrol* **45:** 473-483 DOI:10.1159/000475890.

527 **Pan WM, Wang H, Zhang XF, Xu P, Wang GL, Li YJ, Huang KP, Zhang YW, Zhao
528 H, Du RL, Huang H, Zhang XD, Zhang JX. 2020.** miR-210 Participates in Hepatic Ischemia
529 Reperfusion Injury by Forming a Negative Feedback Loop With SMAD4. *Hepatology* **72:** 2134-
530 2148 DOI:10.1002/hep.31221.

531 **Schrier RW, Wang W. 2004.** Acute renal failure and sepsis. *N Engl J Med* **351:**159-69
532 DOI:10.1056/NEJMra032401.

533 **Shapiro MD, Bagley J, Latz J, Godwin JG, Ge XP, Tullius SG, Iacomini J. 2011.**
534 MicroRNA expression data reveals a signature of kidney damage following ischemia reperfusion
535 injury. *PLoS One* **6:** e23011 DOI:10.1371/journal.pone.0023011.

536 **Sonoda H, Lee BR, Park KH, Nihalani D, Yoon JH, Ikeda M, Kwon SH. 2019.** miRNA
537 profiling of urinary exosomes to assess the progression of acute kidney injury. *Sci Rep* **9:** 4692
538 DOI:10.1038/s41598-019-40747-8.

539 **Srirussamee K, Mobini S, Cassidy NJ, Cartmell SH. 2019.** Direct electrical stimulation
540 enhances osteogenesis by inducing Bmp2 and Spp1 expressions from macrophages and
541 preosteoblasts. *Biotechnol Bioeng* **116:** 3421-3432 DOI:10.1002/bit.27142.

542 **Thul PJ, Åkesson L, Wiking M, Mahdessian D, Geladaki A, Ait BH, Alm T, Asplund
543 A, Björk L, Breckels LM, Bäckström A, Danielsson F, Fagerberg L, Fall J, Gatto L, Gnann
544 C, Hober S, Hjelmare M, Johansson F, Lee S, Lindskog C, Mulder J, Mulvey CM, Nilsson
545 P, Oksvold P, Rockberg J, Schutten R, Schwenk JM, Sivertsson Å, Sjöstedt E, Skogs M,
546 Stadler C, Sullivan DP, Tegel H, Winsnes C, Zhang C, Zwahlen M, Mardinoglu A, Pontén
547 F, von Feilitzen K, Lilley KS., Uhlén M, Lundberg E. 2017.** A subcellular map of the human
548 proteome. *Science* **356:** aal3321 DOI:10.1126/science.aal3321.

549 **Tilney NL, Guttmann RD. 1997.** Effects of initial ischemia/reperfusion injury on the
550 transplanted kidney. *Transplantation* **64:** 945-7 DOI:10.1097/00007890-199710150-00001

551 **Tobisawa T, Yano T, Tanno M, Miki T, Kuno A, Kimura Y, Ishikawa S, Kouzu H,
552 Nishizawa K, Yoshida H, Miura T. 2017.** Insufficient activation of Akt upon reperfusion

553   because of its novel modification by reduced PP2A-B55α contributes to enlargement of infarct
554   size by chronic kidney disease. *Basic Res Cardiol* **112:** 31 DOI:10.1007/s00395-017-0621-6.
555   **Tong Z, Cui QH, Wang J, Zhou Y. 2019.** TransmiR v2.0: an updated transcription factor-
556   microRNA regulation database. *Nucleic Acids Res* **47:** D253-D258. DOI:10.1093/nar/gky1023.
557   **Wang L, Li CY, Guan C, Zhang Y, Yang CY, Zhao L, Luan H, Zhou B, Che L, Wang**
558   **YF, Zhang W, Zhang H, Man XF, Jiang W, Xu Y. 2021.** Nicotiflorin attenuates cell apoptosis
559   in renal ischemia-reperfusion injury through activating transcription factor 3. *Nephrology* **26:**
560   358-368 DOI:10.1111/nep.13841.
561   **Wang YY, Men M, Yang WN, Zheng H, Xue S. 2015.** MiR-31 Downregulation Protects
562   Against Cardiac Ischemia/Reperfusion Injury by Targeting Protein Kinase C Epsilon (PKCε)
563   Directly. *Cell Physiol Biochem* **36:** 179-90 DOI:10.1159/000374062.
564   **Wu HY, Huang T, Ying L, Han CH, Li DW, Xu Y, Zhang M, Mou S, Dong Z. 2016.**
565   MiR-155 is Involved in Renal Ischemia-Reperfusion Injury via Direct Targeting of FoxO3a and
566   Regulating Renal Tubular Cell Pyroptosis. *Cell Physiol Biochem* **40:** 1692-1705
567   DOI:10.1159/000453218.
568   **Yan Y, Ma ZW, Zhu JF, Zeng MR, Liu H, Dong Z. 2020.** miR-214 represses mitofusin-2
569   to promote renal tubular apoptosis in ischemic acute kidney injury. *Am J Physiol Renal Physiol*
570   **318:** F878-F887 DOI:10.1152/ajprenal.00567.2019.
571   **Yang JR, Chen KH, Huang K, Fu BQ, Lin LR, Zhang JG, Li KL, He YN. 2017.**
572   Transcription Factor Trps1 Promotes Tubular Cell Proliferation after Ischemia-Reperfusion
573   Injury through cAMP-Specific 3',5'-Cyclic Phosphodiesterase 4D and AKT. *J Am Soc Nephrol*
574   **28:** 532-544 DOI:10.1681/ASN.2016010009.
575   **Yip HK, Yang CC, Chen KH, Huang TH, Chen YL, Zhen YY, Sung PH, Chiang HJ,**
576   **Sheu JJ, Chang CL, Chen CH, Chang HW, Chen YT. 2015.** Combined melatonin and
577   exendin-4 therapy preserves renal ultrastructural integrity after ischemia-reperfusion injury in the
578   male rat. *J Pineal Res* **59:** 434-47 DOI:10.1111/jpi.12273.
579   **Yuan XP, Wang XP, Chen CB, Zhou J, Han M. 2017.** Bone mesenchymal stem cells
580   ameliorate ischemia/reperfusion-induced damage in renal epithelial cells via microRNA-223.
581   *Stem Cell Res Ther* **8:** 146 DOI:10.1186/s13287-017-0599-x.
582   **Yue JN, Si Y, Zhu T, Yang J, Xu X, Fang Y, Fu WG. 2019.** MicroRNA-187 Reduces
583   Acute Ischemic Renal Podocyte Injury via Targeting Acetylcholinesterase. *J Surg Res* **244:** 302-
584   311. DOI:10.1016/j.jss.2019.06.005.
585   **Zhang LL, Xu Y, Xue S, Wang XD, Dai HL, Qian JQ, Ni ZH, Yan YC. 2017.**
586   Implications of dynamic changes in miR-192 expression in ischemic acute kidney injury. *Int*
587   *Urol Nephrol* **49:** 541-550 DOI:10.1007/s11255-016-1485-7.
588   **Zhang RX, Zhu Y, Li Y, Liu WZ, Yin L, Yin SQ, Ji C, Hu YY, Wang QN, Zhou XR,**
589   **Chen JY, Xu WR, Qian H. 2020.** Human umbilical cord mesenchymal stem cell exosomes
590   alleviate sepsis-associated acute kidney injury via regulating microRNA-146b expression.
591   *Biotechnol Lett* **42:** 669-679 DOI:10.1007/s10529-020-02831-2.

592   **Zhou GY, Soufan O, Ewald J, Hancock REW, Basu N, Xia JG. 2019.** NetworkAnalyst
593   3.0: a visual analytics platform for comprehensive gene expression profiling and meta-analysis.
594   *Nucleic Acids Res* **47:** W234-W241 DOI:10.1093/nar/gkz240.
595   **Zhou YY, Zhou B, Pache L, Chang M, Khodabakhshi AH, Tanaseichuk O, Benner C,**
596   **Chanda SK. 2019.** Metascape provides a biologist-oriented resource for the analysis of systems-
597   level datasets. *Nat Commun* **10:** 1523 DOI:10.1038/s41467-019-09234-6.
598   **Zhu GM, Pei LJ, Lin F, Yin HB, Li XY, He WY, Liu N, Gou X. 2019.** Exosomes from
599   human-bone-marrow-derived mesenchymal stem cells protect against renal ischemia/reperfusion
600   injury via transferring miR-199a-3p. *J Cell Physiol* **234:** 23736-23749 DOI:10.1002/jcp.28941.
601

Details of the included microarray datasets.

IRI, Ischemia reperfusion injury; Ctrl, Control.

1 **Table 1:**

2 **Details of the included microarray datasets.**

GSE ID	Samples (IRI vs Ctrl)	Platform	Year	Type
GSE39548	12 vs 8	GPL7202	2012	mRNA
GSE52004	26 vs31	GPL6246	2014	mRNA
GSE71647	4 vs 4	GPL7202	2016	mRNA
GSE87024	21 vs 9	GPL6887	2016	mRNA
GSE131288	6 vs 6	GPL16570	2019	mRNA
GSE29495	8 vs 8	GPL13642	2011	miRNA

Details of the negative feedback loops in renal IRI

IRI, Ischemia reperfusion injury; TF, transcription factor; SRAID indicates the source of evidence.

1 **Table 2:**

2 **Details of four negative feedback loops in renal IRI.**

TF	miRNA name	Binding site	SRAID	miRNA Sequence	Target Score
Fosl2	mir-155	chr16:84703195-84703369 (score=647)	SRX187214	UUAAUGCUAAUUGUGAUAGGGGU	73
Fosl2	mir-146a	chr11:43377227-43377530 (score=541)	SRX187215	UGAGAACUGAAUUCCAUGGGUU	51
Mafk	mir-25	chr5:138165696-138165895 (score=1000)	SRX188829	CAUUGCACUUGUCUCGGUCUGA	71
Cebpb	mir-155	chr16:84712939-84713250 (score=447)	SRX2901279	UUAAUGCUAAUUGUGAUAGGGGU	88

Figure 1

Flowcharts of the study for analyzing TFs-miRNA-mRNA pathways network.

IRI, ischemia reperfusion injury; DEGs, differentially expressed genes; RRA, RobustRankAggreg; GO, gene ontology; KEGG, Kyoto Encyclopedia of Genes and Genomes; DEMs, differentially expressed miRNAs; TF, transcription factor; PPI, protein-protein interaction.
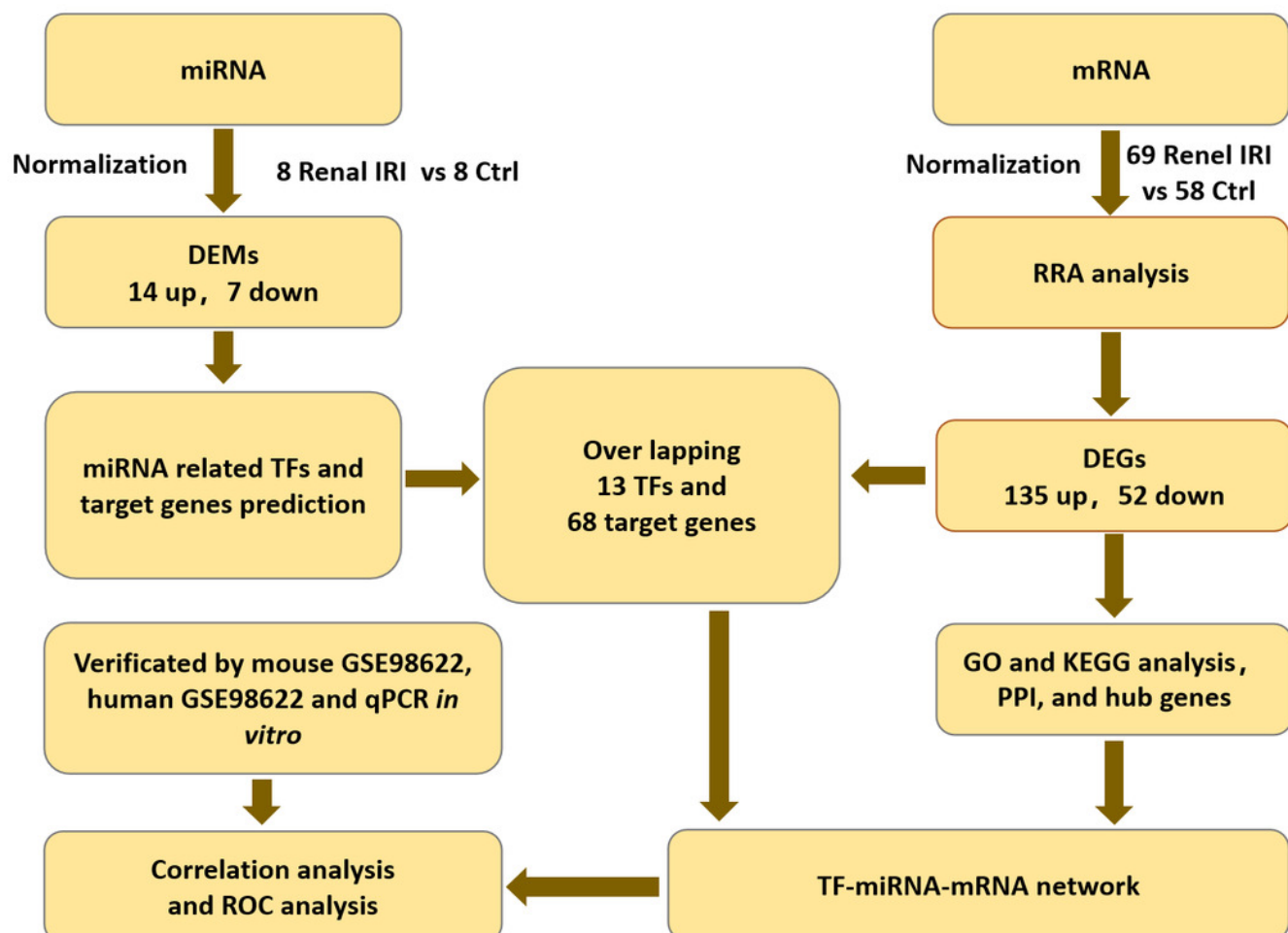
Figure 2

Heatmap of DEMs and DEGs expression profiles between renal IRI mice and controls.

(A) The heatmap showed 21 DEMs between renal tissues from renal IRI mice and controls. Each row represents different miRNA, and each column represents different sample from GSE29495. The samples on the right side of the cluster were renal IRI group. (B) Heatmap of the top 20 down and up-regulated DEGs from renal IRI mice in the result of RRA analysis. Each row represents different DEG, and each column represents different gene expression profile, indicating the consistency of DEGs in different gene expression profile. Red in the heatmap indicates high expression of miRNA or genes, while green represents low expression.
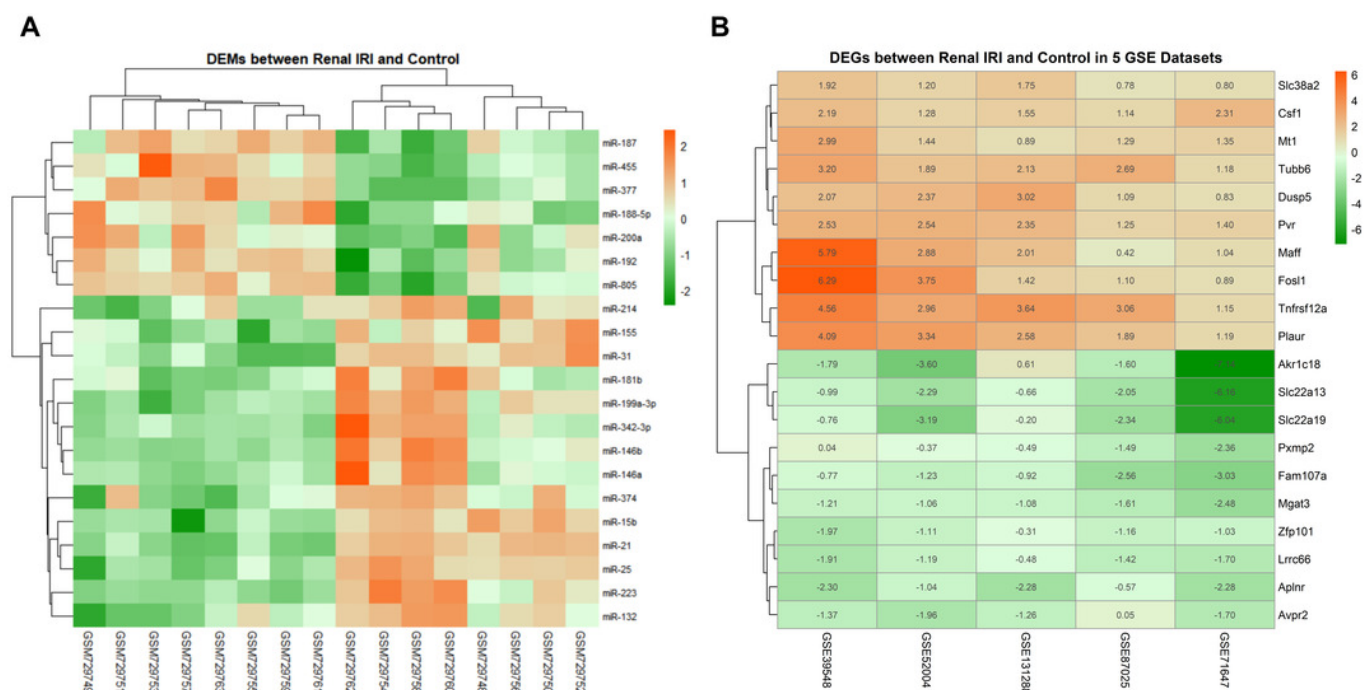
Figure 3

Functional enrichment analysis of RRA DEGs and construction of PPI network.

(A) Bar graph for GO and KEGG enrichment analysis of RRA DEGs, one per cluster, using *p*<0.05 to represent statistical significance. (B) Enrichment network clusters of RRA DEGs showing the connection and similarities between enriched terms. (C) The PPI network of DEGs associated with renal IRI. The red, blue and green modules showing their close connection in the network. (D) Modules in MCODE analysis were considered as hub genes and were marked in red, blue and green.
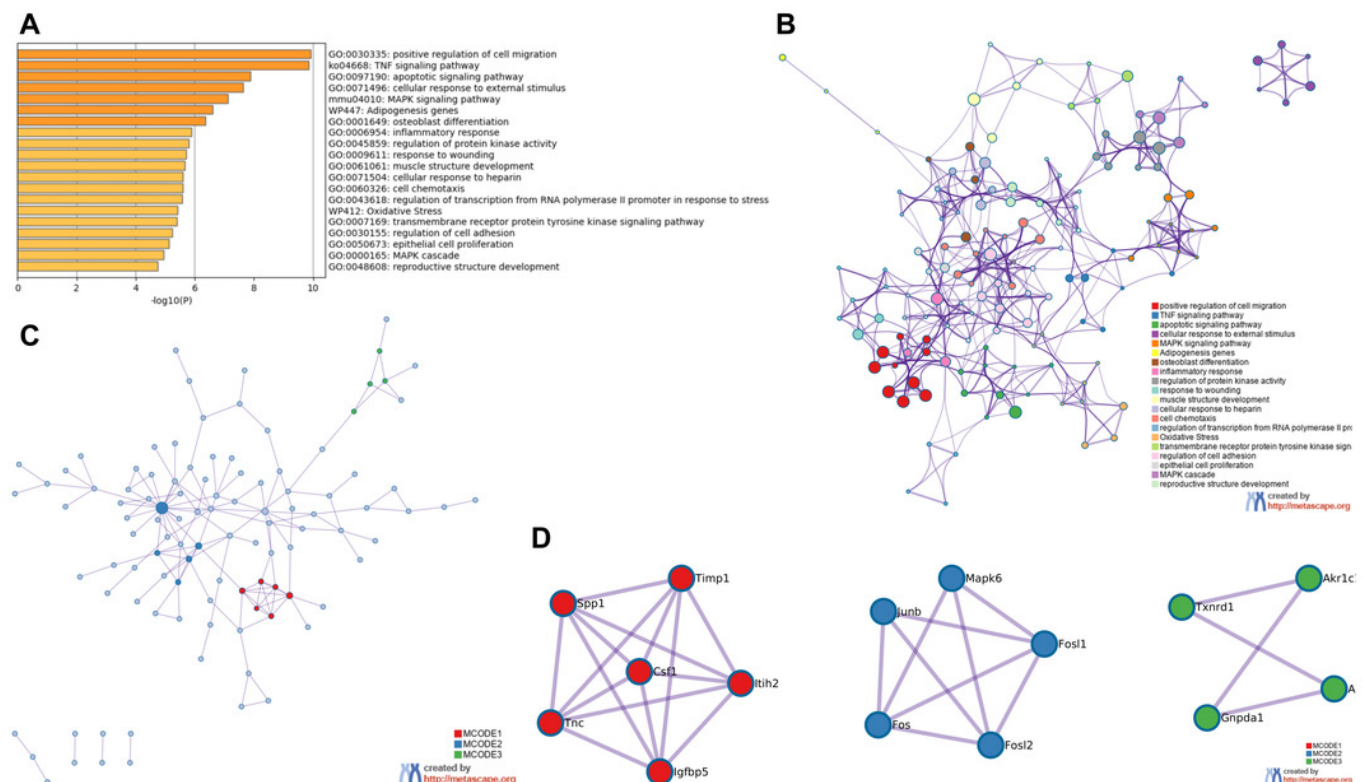
Figure 4

Construction of TFs-miRNA-mRNA pathways network associated with renal IRI.

(A) Venn diagram of TFs and RRA DEGs showed differentially expressed TFs. TFs were obtained according to TransmiR v2.0 database. (B) Venn diagram of RRA DEGs and target genes of DEMs showed differentially expressed target genes. Target genes of DEMs were predicted by miRDB and finally 68 genes were identified. The red target genes indicate that they are also transcription factors. (C) Construction of TF-miRNA-mRNA pathways network. The squares indicate differentially expressed TFs, the butterflies indicate differentially expressed miRNAs, the circles indicate differentially expressed target genes. The solid line indicates activation relationship between TFs and miRNAs. The dotted line indicates inhibition relationship between miRNAs and their target genes. 11 TFs, 10 miRNA and 17 target genes were incorporated into the network because they were accord with the regulatory relationship, and other genes were deleted because they were not accord with the regulatory relationship.

A

TFs

261

174

RRA DEGs

Atf4
Cebpb
Egr1
Egr2
Fos
Fosl1
Fosl2
Junb
Mafk
Nfil3
Snai1
Sox4
Sox9

B

Target genes

6899

68

119

RRA DEGs

Up regulated
Cebpb
Fos
Fosl2
Fosl1
Mafk
Sox9
Cxadr
Plaur
Mthfd2
Dusp8
Emp1
......

Down regulated
Zfp467
Ranbp3l
Galm
Sfrp1
Ass1
Cyp7b1
Crebl2
A4gnt
Aplnr
Zfp760
......

C
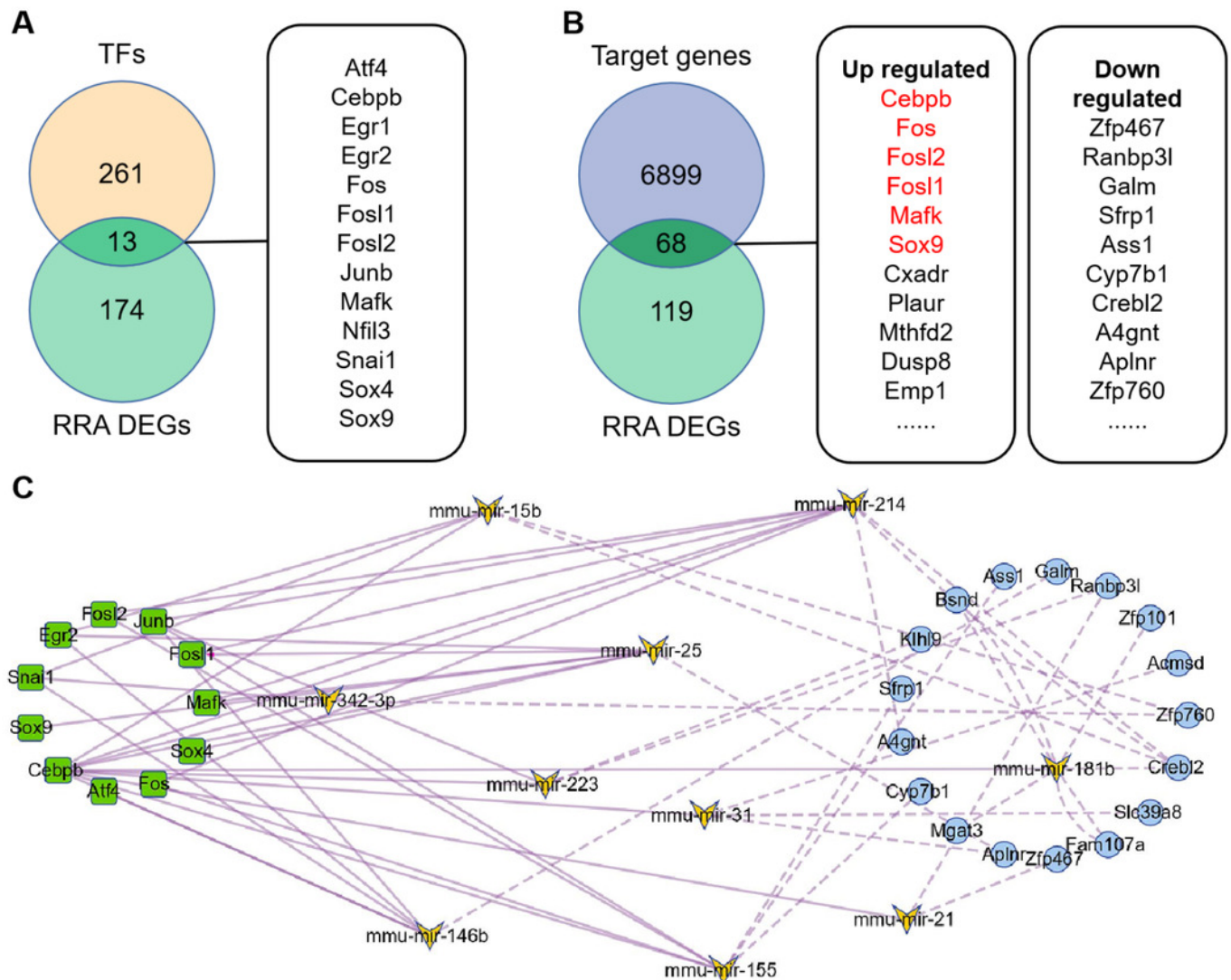
Figure 5

Diagnostic value of hub genes and Correlation coefficient between TFs and target genes.

(A) Correlation analysis between differentially expressed TFs and differentially expressed target genes in the network. The frames marked in red and blue indicate regulatory relationship between TFs and targets. The red frame in the lower left corner indicates correlation, and the blue frame indicates no correlation. (B) Diagnostic value of hub genes and genes from the network in renal IRI in GSE52004.
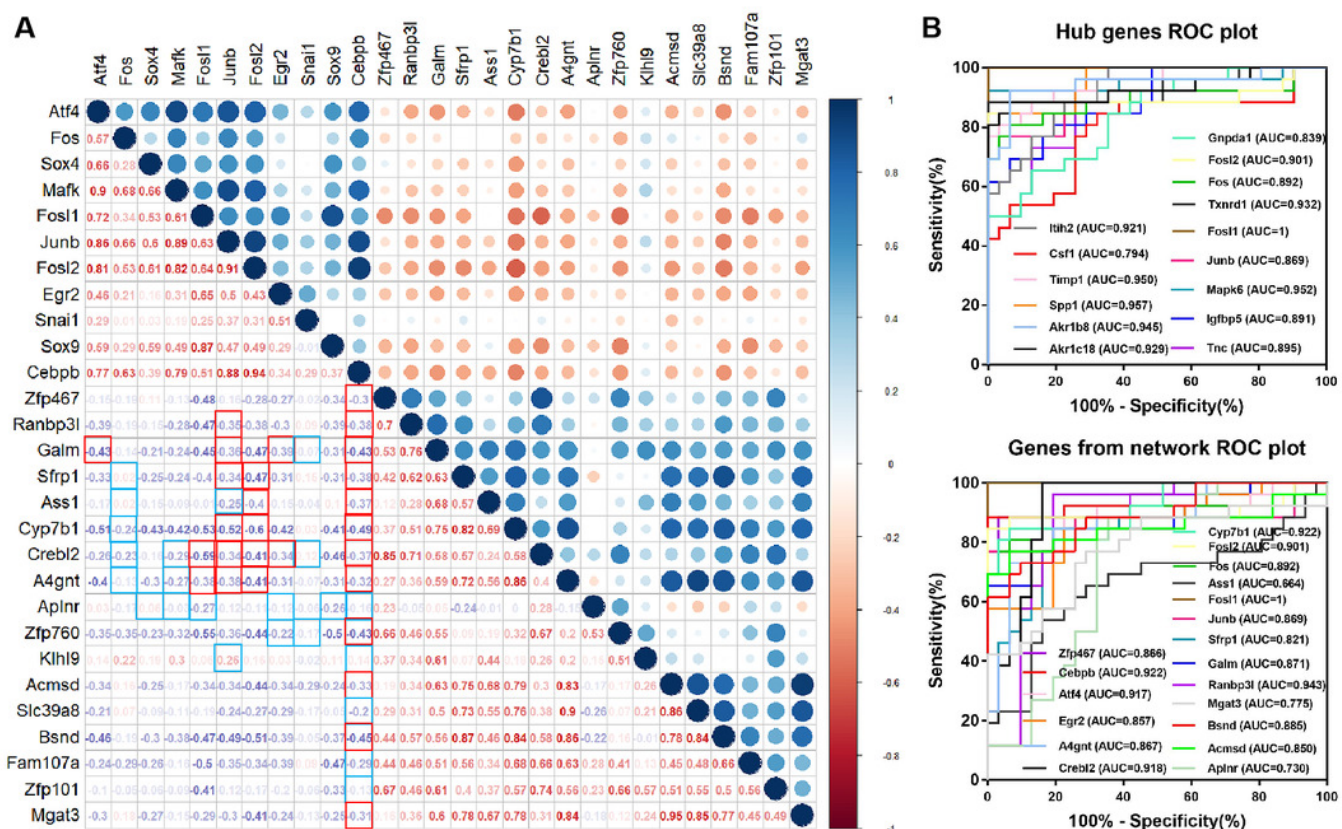
Figure 6

Verification of the expression of genes and their diagnostic value, and correlation between the genes in mice RNA-seq datasets GSE98622 and human datasets GSE134386.

(A) Relative mRNA expression of hub genes and genes from the network in GSE98622. TFs were marked in green, target genes were marked in orange. (B) Correlation analysis between TFs and target genes from the network in GSE98622. Black indicates irrelevant again; Red indicates relevant again; Green indicates that the two results were inconsistent. (C) Diagnostic value of hub genes and genes from the network in renal IRI in GSE98622. (D) Relative mRNA expression of hub genes and genes from the network in human, which were also differently expressed in mouse samples.
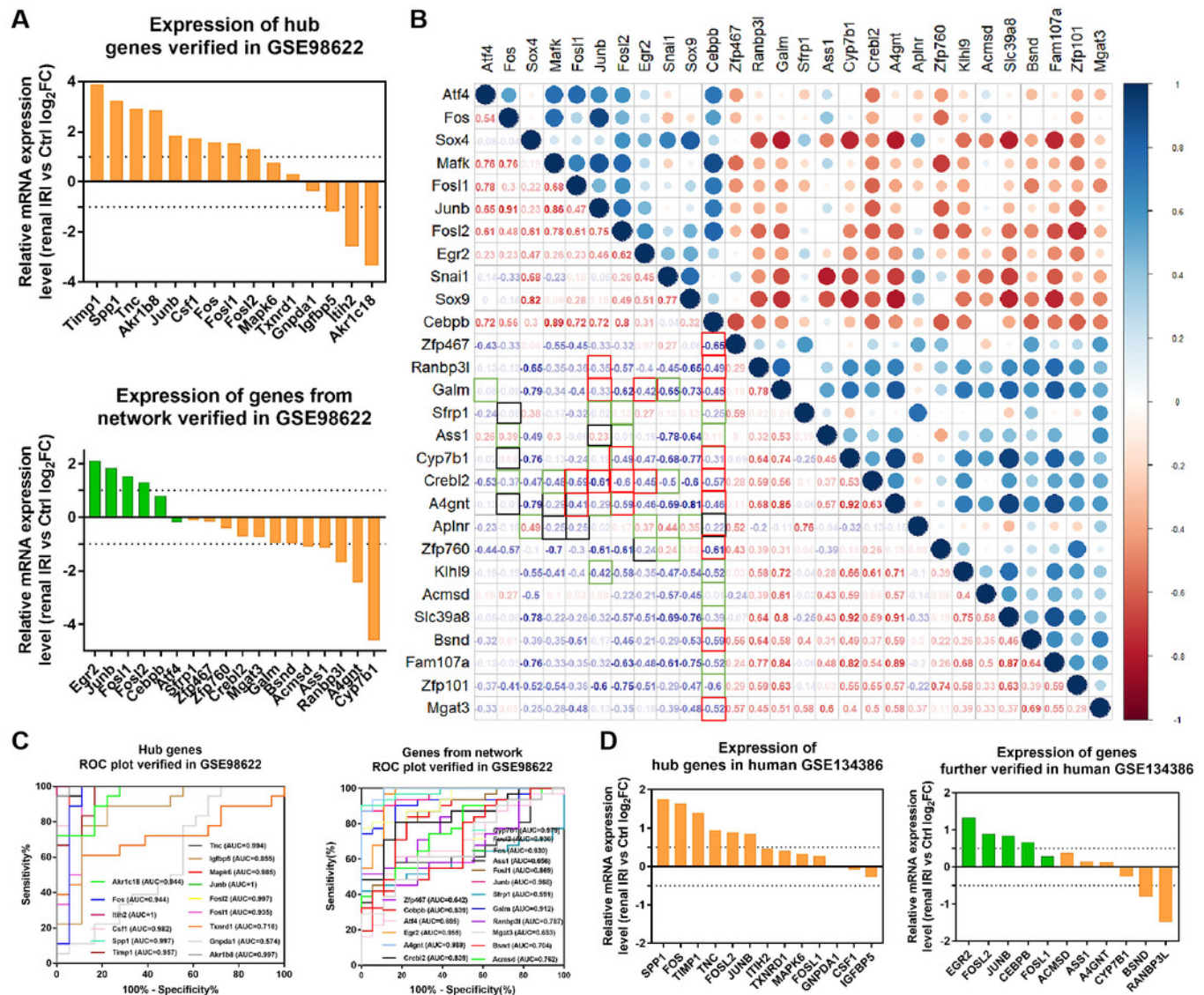
Figure 7

Verification of the expression of genes *in vitro*.

(A) The expression of Bsnd in normal kidney tissues. The orange modules show that the Bsnd and Ranbp3l are highly expressed in normal kidney. Downloaded from The Human Protein Atlas. (B) Immunohistochemical staining showed that Bsnd and Ranbp3l were highly expressed in normal kidney tissues. Left, Bsnd; right, Ranbp3l. Downloaded from The Human Protein Atlas. (C) The expression of genes in HK-2 HR model *in vitro*. (D) Bsnd and Ranbp3l were up-regulated after knockdown of Cebpb *in vitro*.

A

Consensus dataset[i]

RNA tissue specificity: Group enriched (blood, kidney, salivary gland)

| Organ | **Expression** | **Alphabetical** |

mRNA expression of Bsnd
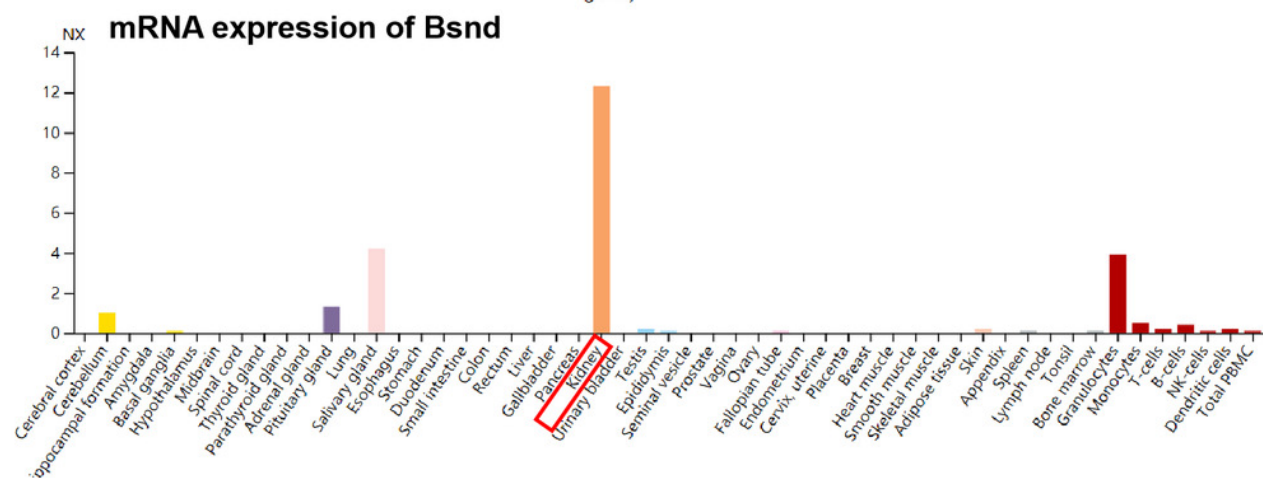
Consensus dataset[i]

RNA tissue specificity: Tissue enhanced (brain, kidney)

| Organ | **Expression** | **Alphabetical** |

mRNA expression of Ranbp3l
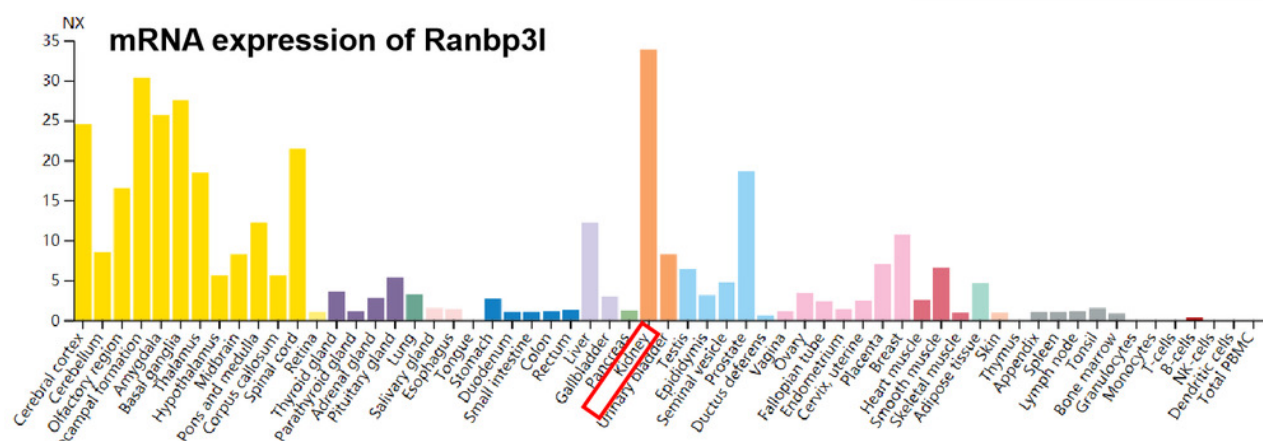
B
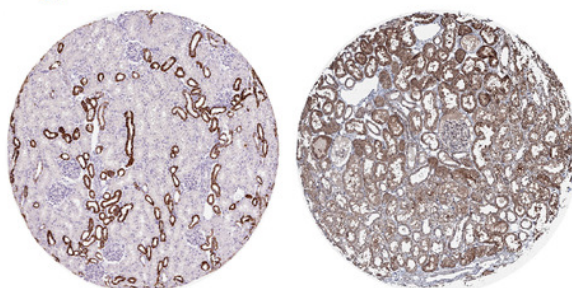
C Renal IRI vs Ctrl
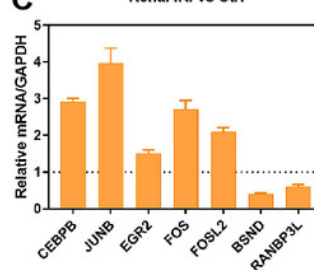
D Knockdown of CEBPB vs IRI